

1

2 Bayesian Estimation of the Transmissivity Spatial Structure from Pumping
3 Test Data

4

5 Mehmet Taner Demir¹, Nadim K Copty¹, Paolo Trincherò², Xavier Sanchez-Vila³

6

7 ¹ Institute of Environmental Sciences, Bogazici University, Istanbul, 34342 Turkey

8 ² AMPHOS 21 Consulting S.L., Passeig de García i Faria, 49-51, 1 – 1 E08019 – Barcelona,
9 Spain

10 ³ Department of Civil and Environmental Engineering, Universitat Politecnica de Catalunya
11 - UPC, Jordi Girona 31, 08034 Barcelona, Spain

12

13

ABSTRACT

14

15

16

17

18

19

20

21

22

23

24

25

26

27

28

29

30

31

32

33

34

35

Estimating the statistical parameters (mean, variance, and integral scale) that define the spatial structure of the transmissivity or hydraulic conductivity fields is a fundamental step for the accurate prediction of subsurface flow and contaminant transport. In practice, the determination of the spatial structure is a challenge because of spatial heterogeneity and data scarcity. In this paper, we describe a novel approach that uses time drawdown data from multiple pumping tests to determine the transmissivity statistical spatial structure. The method builds on the pumping test interpretation procedure of Coptý et al. (2011) (Continuous Derivation method, CD), which uses the time-drawdown data and its time derivative to estimate apparent transmissivity values as a function of radial distance from the pumping well. A Bayesian approach is then used to infer the statistical parameters of the transmissivity field by combining prior information about the parameters and the likelihood function expressed in terms of radially-dependent apparent transmissivities determined from pumping tests. A major advantage of the proposed Bayesian approach is that the likelihood function is readily determined from randomly generated multiple realizations of the transmissivity field, without the need to solve the groundwater flow equation. Applying the method to synthetically-generated pumping test data, we demonstrate that, through a relatively simple procedure, information on the spatial structure of the transmissivity may be inferred from pumping tests data. It is also shown that the prior parameter distribution has a significant influence on the estimation procedure, given the non-uniqueness of the estimation procedure. Results also indicate that the reliability of the estimated transmissivity statistical parameters increases with the number of available pumping tests.

36 1. INTRODUCTION

37 The modeling of groundwater flow and contaminant transport has evolved in recent decades
38 into a valuable tool for the analysis of subsurface systems. Such modeling efforts require
39 mapping the flow parameters - most notably transmissivity (T) or hydraulic conductivity (K)
40 - over the domain of interest. Numerous field investigations have however demonstrated that
41 hydrogeological parameters are highly heterogeneous, displaying complex patterns of spatial
42 variability (e.g., *Gelhar* 1993; *Rubin*, 2003, *Sudicky et al.* 2010). Because flow and transport
43 are strongly influenced by the heterogeneity of the subsurface system, incorporating the
44 spatial variability of the underlying parameters is essential for the accurate evaluation of
45 groundwater resources, and in particular for the prediction of contaminant transport as a
46 necessary step for the design and implementation of groundwater remediation activities (e.g.,
47 *Sanchez-Vila and Fernandez-Garcia*, 2016).

48 Complexity in hydrogeological patterns and the lack of detailed data have led researchers to
49 formulate the flow and transport problem within a stochastic framework. With such an
50 approach, flow parameters are defined by spatial random functions whose spatial structure
51 can adequately be expressed in terms of few low-order statistical parameters, namely the
52 spatial mean, variance, and integral scale, which jointly define the covariance function or
53 semi-variogram (*Kitanidis*, 1997; *Renard*, 2007). These statistical parameters are typically
54 determined from measurements of the attribute of interest, provided that a sufficiently large
55 number of data with adequate spatial coverage is available.

56 Groundwater flow and solute transport are strongly affected by the spatial distribution of T .
57 At most sites, the number of T estimates determined from the interpretation of pumping tests
58 is quite limited, hindering the accurate determination of the T covariance function.
59 Moreover, traditional pumping test interpretation methods, such as those based on log-log
60 plots (*Theis*, 1935) or semilog plots (*Cooper and Jacob*, 1946), generally yield single
61 estimates of the flow parameters, which hardly provide information about the underlying
62 heterogeneity. In fact, this averaging process results in T estimates with a smaller variance
63 and a larger integral scale as compared to the actual point distributions, and hence, cannot
64 be used to simulate the impact of small to medium scale variability, which is of interest in
65 many field applications.

66 These limitations motivated many researchers in the last three decades to examine the impact
67 of spatial heterogeneity on the analysis of pumping tests and investigate whether information
68 about the spatial variability of the flow parameters can be inferred from pumping tests (a

69 review of methods and solutions was provided by *Sanchez-Vila et al.*, 2006). A very early
70 study is *Barker and Herbert* (1982), who considered the effect of a high hydraulic
71 conductivity anomaly embedded in an otherwise uniform aquifer. *Butler* (1988) used the
72 *Cooper and Jacob* (1946) method to investigate the effect of a T anomaly on the interpreted
73 transmissivity; it was shown that, for observation wells located at large distances from the
74 pumping well, the perturbed non-uniform aquifer behaves as a homogeneous aquifer. On the
75 other hand, *Butler* (1990) showed that the T values estimated with the *Theis* (1935) method
76 place more weight on the local T , defined as the T in the vicinity of the pumping well. *Feitosa*
77 *et al.* (1994) developed an inverse procedure for the estimation of the transmissivity as a
78 function of distance from the pumping well for the case when the transmissivity field
79 consists of a series of concentric homogeneous rings.

80 For spatially variable T fields (i.e., T fields that are not defined in terms of a deterministic
81 perturbation but that are individual realizations of a random field), *Meier et al.* (1998) and
82 *Sanchez-Vila et al.* (1999) showed that the transmissivity obtained with the *Cooper and*
83 *Jacob* (1946) is close to the spatial geometric mean of the T field, regardless of the location
84 of the observation point. On the other hand, the estimated storativity (S) varies spatially,
85 demonstrating how the interpretation method significantly translates the heterogeneity in
86 transmissivity into spatially variable S estimates. This finding was further confirmed by
87 *Trincherro et al.* (2008b), who provided an analytical relationship between the estimated
88 storativity and the porosity inferred from tracer test data (the latter parameter was considered
89 as an indicator of transport connectivity).

90 *Coptý and Findikakis* (2004a) examined the sensitivity of transient drawdown in pumping
91 tests to the statistical parameters describing the spatial structure of T , and noted that the time
92 derivative of the drawdown is particularly sensitive to the heterogeneity in T . *Oliver* (1993)
93 and *Knight and Kluitenberg* (2005) used the Frechet kernel to evaluate the sensitivity of the
94 drawdown to the spatial variability of T and S . *Leven and Dietrich* (2006) used sensitivity
95 coefficients to assess the influence of the spatial variability of T and S on the interpretation
96 of pumping tests, leading to time-dependent interpreted parameters. *Avci et al.* (2011, 2013)
97 developed a numerical method for the estimation of the variability of the T and S as a
98 function of pumping time; the method could be used as a diagnostic tool to identify some
99 aquifer system characteristics. *Avci et al.* (2014) evaluated the performance of a number of
100 analytical methods for the estimation of the variation of the transmissivity with radial
101 distance. Recently, *Pechstein et al.* (2016) discussed the relationship of the interpreted T

102 values derived from pumping tests to the underlying spatial variability of the T field. The
103 authors showed numerically that the interpreted T value that best reproduces the pumping
104 test data in confined heterogeneous aquifers is a weighted average of the point T values
105 which uses the temporal derivative of the Frechet kernel as a spatial weight.

106 *Copty et al. (2008)* and *Trincherio et al. (2008a)* considered the influence of spatial variability
107 of the transmissivity on pumping tests conducted in leaky aquifers. A significant difference
108 between flow towards a well in a confined non-leaky versus a leaky aquifer is that in the
109 former case the cone of depression continues to expand with time, while in the latter a steady
110 state condition is reached. As a result, the response of a pumping test in a leaky aquifer is
111 more sensitive to variations in the local transmissivity in the vicinity of the well, as compared
112 to the case of a confined aquifer.

113 A number of studies have attempted to estimate directly, from pumping test data, the
114 statistical spatial structure of the transmissivity field, commonly expressed in terms of two
115 statistical parameters: variance and integral scale. *Copty and Findikakis (2004b)* examined
116 the relation of the time-derivative of the drawdown to the integral scale and the variance of
117 the log-transmissivity field. *Neuman et al. (2004, 2007)* developed a graphical approach that
118 uses steady-state drawdown data for the estimation of the T variance and integral scale. *Riva*
119 *et al. (2009)* applied this type-curve method to field data from the site of Poitiers, France.
120 *Firmani et al. (2006)* used an expression of the equivalent hydraulic conductivity for steady-
121 state radially convergent flow towards a well in a heterogeneous aquifer to estimate the
122 variance and integral scale of K . *Zech et al. (2012)* developed an analytical expression for
123 the steady state drawdown due to pumping in a heterogeneous aquifer using the Coarse
124 Graining upscaling method (*Attinger, 2003*), a method subsequently applied to real pumping
125 test data from the Horkheimer Insel test site in Germany (*Zech et al., 2015*). This latter paper
126 also discusses the quantity and spatial coverage of the data needed to obtain reliable
127 estimates of the statistical parameters of the transmissivity field. *Zech et al. (2016)* extended
128 the analysis to transient flow and showed that the number of measurements needed to obtain
129 reliable estimates of the transmissivity spatial structure is reduced compared to steady state
130 pumping tests.

131 In parallel efforts, and to overcome the scarcity of hydrological data commonly encountered
132 in field applications, a number of researchers have proposed incorporating additional
133 secondary data in the identification of subsurface parameters such as geophysical data (see
134 recent reviews such as *Binley et al., 2015; Slater, 2007; Rubin and Hubbard, 2005*). Novel

135 field data acquisition techniques, such as hydraulic tomography (e.g., *Butler et al.*, 1999;
136 *Yeh, and Liu*, 2000; *Zhu and Yeh*, 2005; *Yin and Illman*, 2009; *Illman et al.*, 2015) and direct
137 push technologies (*Butler et al.*, 2007; *Dietrich et al.*, 2008; *Bohling et al.*, 2012) have also
138 been proposed. These approaches have been shown to have several benefits; most notably
139 they allow for the collection of dense hydraulic head data in response to groundwater
140 pumping that allows for the estimation of the three-dimensional hydraulic conductivity
141 distribution in the vicinity of the tests. Despite these advantages, their application to routine
142 field problems remains limited due to the relatively large costs associated and the difficulty
143 of solving the groundwater inverse problem.

144 Despite these recent developments, the determination of the underlying statistical spatial
145 structure of the transmissivity field from pumping test data remains a challenge. In a recent
146 study, *Copty et al.* (2011) developed an interpretation method for pumping tests, denoted as
147 the Continuous Derivation (CD) method. The CD method uses the transient drawdown data
148 and its time derivative to estimate interpreted transmissivities as a function of the radial
149 distance, $T_i(r)$. It was shown by *Copty et al.* (2011) that $T_i(r)$ is close to the geometric mean
150 of the T values over a radially increasing volume, $T_g(r)$. The function $T_g(r)$ varies from the
151 transmissivity at the well for small values of r , to the geometric mean of the entire field, for
152 large r values. In the current study, we extend the work of *Copty et al.* (2011) by examining
153 whether $T_i(r)$ can be used to infer the spatial structure of the transmissivity field. The goal is
154 thus to develop a relatively simple pumping test interpretation method that can help in the
155 definition of relevant characteristics of the local scale transmissivity spatial structure without
156 the need for complex inverse modeling. We primarily focus on time-drawdown data derived
157 from pumping tests, which remains a widely used technique for subsurface parameter
158 estimation.

159 For the sake of completion, we present in Section 2 the main features of the CD method,
160 followed by the presentation of the Bayesian approach used to infer the spatial structure of
161 the transmissivity field, namely the variance and the integral scale. Section 3 describes a
162 numerical application of the proposed Bayesian method and discusses its potential
163 applications and limitations.

164

165 **2. Pumping Test Interpretation Method**

166 **2.1. The Continuous Derivation Method (CD)**

167 For pumping tests conducted in heterogeneous aquifers, the cone of depression due to
 168 pumping expands in time. At early times the apparent transmissivity is close to the T value
 169 in the immediate vicinity of the well (order of few meters), while at later times it is some
 170 weighted average of the transmissivity of a much larger region around the well. The term
 171 “apparent” is used here in accordance with the terminology of *Sanchez-Vila et al.*, 2006
 172 which refers to an estimate of the parameter that is function of space and that satisfies some
 173 relationship such as the Theis solution (*Theis*, 1935). The CD method (*Copty et al.*, 2011)
 174 captures the full temporal transition between the local T value and the estimate obtained
 175 using late time data. The estimation method relies on the time-derivative of the drawdown
 176 because this is more sensitive than the drawdown itself to spatial variation of transmissivity
 177 (e.g., *Bourdet*, 2002).

178 For two-dimensional flow towards a well in a confined aquifer, the time-dependent
 179 drawdown is given by the classical Theis’ solution: $s(t, r) = \frac{Q}{4\pi T} W(u)$, where $u = \frac{r^2 S}{4tT}$,
 180 $W(u)$ is the well (i.e., the exponential integral) function, Q is the pumping rate, r is the
 181 separation distance between the pumping and observation wells, t is time, and S is storativity.
 182 The ratio of the drawdown to the drawdown time derivative, $s'(t, r)$, can be written as (*Copty*
 183 *et al.*, 2011):

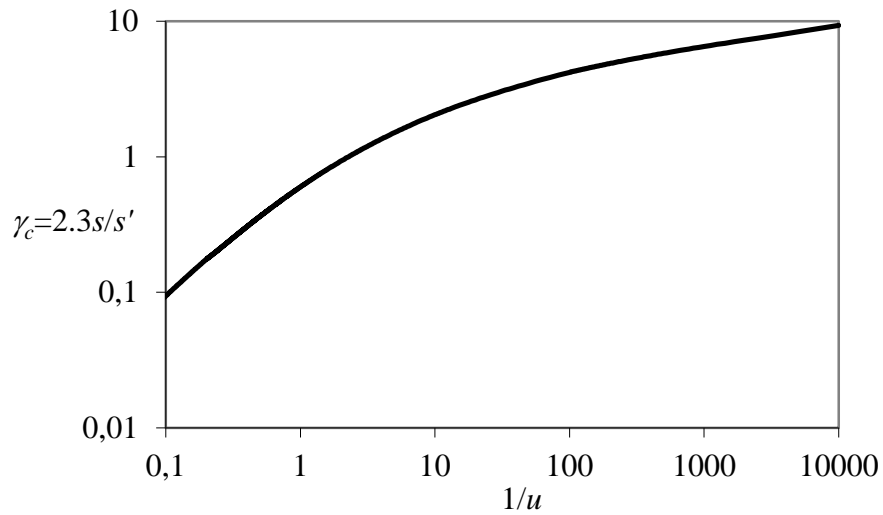
$$184 \quad \gamma_c = \frac{2.3s}{s'} = W(u) \exp(u) \quad (1)$$

185
 186 A plot of the function γ_c is shown in Figure 1. It is observed that γ_c increases monotonically
 187 with dimensionless $1/u$ (equivalent to a dimensionless time). For a given pumping test, the
 188 ratio of the observed drawdown at any time t to its time derivative provides an estimate of u
 189 from (1). From the estimated u value, the interpreted transmissivity and storativity (T_i and
 190 S_i , respectively) corresponding to that particular moment in time are then estimated as:

$$191 \quad T_i(t) = \frac{Q}{4ps(t)} W(u); \quad S_i(t) = \frac{4tT_i u}{r^2} \quad (2)$$

192 Applying the above procedure repetitively to the full duration of the test yields time-
 193 dependent estimates of the flow parameters. Thus, the CD method provides estimates of the
 194 flow parameters that change with time, in contrast to conventional methods (e.g., the Theis
 195 method) that lump all observed drawdown together to estimate single representative values
 196 of T and S .

197



198

199 Figure 1. Plot of γ_c as a function of $1/u$ (modified from *Copty et al.*, 2011)

200

201 Through sensitivity analysis of the drawdown and its derivative to variations in the
 202 transmissivity, the interpreted transmissivity T_i - t relationship is mapped into a T_i - r^*
 203 relationship, where r^* is a radial distance computed as (*Copty et al.*, 2011):

$$204 \quad r^* = \sqrt{\frac{4tT}{1.65S}}. \quad (3)$$

205 Equation (3) indicates that there is a direct mapping between the values of r^* and t . *Copty et*
 206 *al.* (2011) applied the CD method to synthetically generated 2D aquifers and found that the
 207 curves $T_i(r^*)$ match well to the function $T_g(r)$, defined as the geometric mean of the
 208 transmissivity, computed over a circular area of the aquifer centered around the pumping
 209 well and with radius r . As r increases, $T_g(r)$ approaches the geometric mean of the entire
 210 transmissivity field. Therefore, observation points located at a small distance from the
 211 pumping well (compared to the integral scale of T) would yield the most information about
 212 the spatial variability of T .

213

214

215 **2.2. Bayesian Approach for the Estimation of the Variance and Integral Scale**

216 Since the estimation of the transmissivity variance and integral scale is generally difficult
 217 and therefore associated with a high level of uncertainty, we define these two parameters as
 218 random functions. Denoting V and I as the variance and integral scale random functions,
 219 respectively, the primary goal of this paper is to estimate their conditional joint probability

220 density function (pdf), $f_{V,I}^c(v,i|Y_1 \cdots Y_N)$, where $Y_1 \cdots Y_N$ denotes the drawdown data from N
 221 available pumping tests. The superscript c denotes conditional.

222 Using the CD method, the drawdown data from each pumping test is converted to the
 223 geometric mean of the transmissivity as a function of radial distance from the well, $T_g(r)$.
 224 Interpretation of each pumping test is done separately. If data from more than one
 225 observation well are present for the same pumping test, they would yield similar T estimates
 226 as they would be sampling the same aquifer volume. Under such conditions, it is sufficient
 227 to use data from only one observation well. This redundancy in information has also been
 228 noted by other researchers, such as *Leven and Dietrich (2006)* and *Bohling and Butler*
 229 *(2010)*, who demonstrated the issue of reciprocity of sequential pumping tests when pumping
 230 and monitoring wells are reversed. Limitations of reciprocity have been also explored
 231 elsewhere (e.g., *Delay et al., 2012; Sanchez-Vila et al., 2016*). Substituting each pumping
 232 test by the transmissivity functions derived from the available pumping tests, the conditional
 233 joint pdf is rewritten as $f_{V,I}^c(v,i|T_{g,1}(r) \cdots T_{g,N}(r))$, where $T_{g,1}(r) \cdots T_{g,N}(r)$ denotes the
 234 transmissivity estimates derived from pumping tests $1, \dots, N$. In other words, the goal here can
 235 be restated as the estimation of the joint pdf of V and I conditioned on the estimates of the
 236 geometric mean of the T field as a function of radial distance derived from all available
 237 pumping tests. To simplify the notation, the variable r is dropped from the ensuing
 238 derivations. It is however important to note that $T_{g,k}$ is not a single value but rather a full
 239 function of r .

240 Using Bayes' Theorem on conditional probability (e.g. *Tarantola, 1987*), the joint pdfs are:

$$241 \quad f_{V,I}^c(v,i|Y_1 \cdots Y_N) = f_{V,I}^c(v,i|T_{g,1} \cdots T_{g,N}) = \frac{f_T(T_{g,1} \cdots T_{g,N}|v,i) \times f_{V,I}(v,i)}{f_T(T_{g,1} \cdots T_{g,N})} \quad (4)$$

242 where

243 $f_T(T_{g,1} \cdots T_{g,N}|v,i)$ is the likelihood of observing $T_{g,k}$ given that variance and integral scale
 244 values are v and i , respectively. This pdf can be seen as the reverse of the
 245 desired pdf, $f_{V,I}^c(v,i|T_{g,1} \cdots T_{g,N})$

246 $f_T(T_{g,1} \cdots T_{g,N})$ is the unconditional pdf of observing $T_{g,1} \cdots T_{g,N}$

247 $f_{V,I}(v,i)$ is the prior joint pdf of observing the variance and integral scale values
 248 v and i , respectively.

249 The pdf in the denominator of (4) is denoted as ω , and can be expressed from the definitions
 250 of the marginal and conditional probabilities (Tarantola, 1987) as:

$$251 \quad \omega = f_T(T_{g,1} \cdots T_{g,N}) = \int_{V,I} f_T(T_{g,1} \cdots T_{g,N} | v, i) \times f_{V,I}(v, i) dv di \quad (5)$$

252 In words, the pdf of $T_{g,1} \cdots T_{g,N}$ is equal to the probability of observing $T_{g,1} \cdots T_{g,N}$ given that
 253 $V=v$ and $I=i$, integrated over all possible values of V and I ; ω is a normalizing parameter that
 254 guarantees that (4) is a proper pdf; that is: $\int_{V,I} f_{V,I}^c(v, i | T_{g,1} \cdots T_{g,N}) dv di = 1$

255 If the separation distances between the different pumping tests is large such that the cones
 256 of depression do not significantly overlap (consequently, there is little redundancy in the
 257 data), then the pumping tests can be treated as independent (i.e., they sample different
 258 volumes of the aquifer). The likelihood function $f_T(T_{g,1} \cdots T_{g,N} | v, i)$ can be re-written as a
 259 product of the individual pdfs:

$$260 \quad f_{V,I}^c(v, i | Y_1 \cdots Y_N) = \frac{1}{\omega} f_T(T_{g,1} | v, i) \cdots f_T(T_{g,N} | v, i) f_{V,I}(v, i) \quad (6)$$

261 where

$$262 \quad \omega = \int_{V,I} f_T(T_{g,1} | v, i) \cdots f_T(T_{g,N} | v, i) f_{V,I}(v, i) dv di \quad (7)$$

263 Equation (6) states that the pdf of V and I conditional on the available pumping test data can
 264 be expressed in terms of products of $N+1$ pdfs. The first one, $f_{V,I}(v, i)$, is the prior joint pdf
 265 of V and I , which reflects the level of knowledge of the site *prior* to conducting the pumping
 266 tests. Such information can be derived from previously conducted geologic or geophysical
 267 studies, or adopted from other sites with similar characteristics. In the absence of
 268 information, $f_{V,I}(v, i)$, can be taken as some uniform (uninformative) distribution that
 269 includes all possible values, reflecting the lack of knowledge of the site.

270 The remaining N pdfs are $f_T(T_{g,k} | v, i)$ $k = 1, \dots, N$; i.e., the individual likelihood functions of
 271 observing $T_{g,k}$ given that the aquifer variance and integral scale are v and i , respectively, in
 272 pumping test k . As it will be described in the following subsection, the likelihood functions
 273 can be readily computed without the need for any inverse modeling by generating multiple
 274 realizations of the transmissivity field with different values of V and I , computing the

275 resultant pdf of the geometric mean of the generated transmissivity fields and then evaluating
 276 the likelihood of $T_{g,k}$. Hence, it can be seen that the desired pdf, $f_{V,I}^c(v,i|Y_1 \cdots Y_N)$ depends on
 277 both prior information about the site, $f_{V,I}(v,i)$, and the information derived from the
 278 pumping test, $f_T(T_{g,k}|v,i) k = 1, \dots, N$.

279

280 Finally, the marginal pdfs of V and I are computed as:

$$281 \quad f_V^c(v|Y_1 \cdots Y_N) = \int_I f_{V,I}^c(v,i|Y_1 \cdots Y_N) di, \quad (8)$$

$$282 \quad f_I^c(i|Y_1 \cdots Y_N) = \int_V f_{V,I}^c(v,i|Y_1 \cdots Y_N) dv. \quad (9)$$

283 The expected values of the variance and integral scale can be computed from the integral of
 284 the conditional joint pdf of V and I , $f_{V,I}^c(v,i|Y_1 \cdots Y_N)$:

$$285 \quad E[I] = \int_{V,I} i f_{V,I}^c(v,i|Y_1 \cdots Y_N) dv di, \quad (10)$$

$$286 \quad E[V] = \int_{V,I} v f_{V,I}^c(v,i|Y_1 \cdots Y_N) dv di. \quad (11)$$

287

288 **2.3. Estimation of the likelihood function** $f_T(T_{g,1} \cdots T_{g,N}|v,i)$

289 This section describes the method used to estimate the likelihood function $f_T(T_{g,1} \cdots T_{g,N}|v,i)$

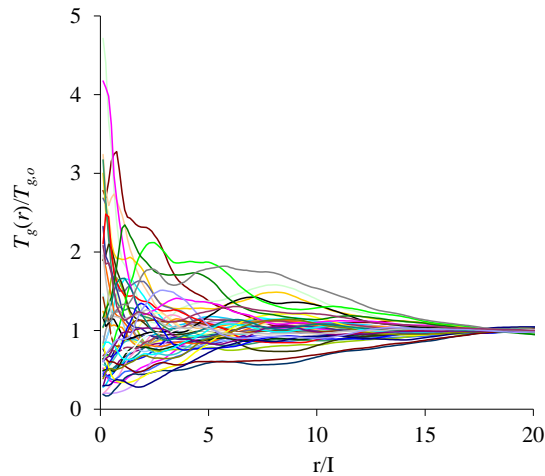
290 . It is assumed that $\ln T$ is a multivariate Gaussian random spatial function with exponential
 291 semi-variogram. Other semi-variogram functions could also be considered. Multiple
 292 realizations ($n=1000$) of the natural logarithm of the transmissivity were randomly generated
 293 for various V and I values using the Turning band method (*Mantoglou and Wilson, 1982*).
 294 The geometric mean of the transmissivity over a circular area with radius r located at the
 295 center of the generated domain was computed as:

$$296 \quad T_g(r) = \exp\left[\int_{r=0}^r \ln(T) dA\right] \quad (12)$$

297 Figure 2 displays $T_g(r)$ for randomly selected transmissivity fields with variance $V=1$. The
 298 radial distance in the figure is normalized by the integral scale, I , while the ensemble
 299 geometric mean, $T_{g,o} = T_g(r \rightarrow \infty)$ was used to normalize the vertical axis. It can be seen

300 that the variability of $T_g(r)$ decreases as r increases. For radial distances larger than about
 301 $20I$, $T_g(r)$ approached the ensemble geometric mean for all of the generated transmissivity
 302 fields.

303



304

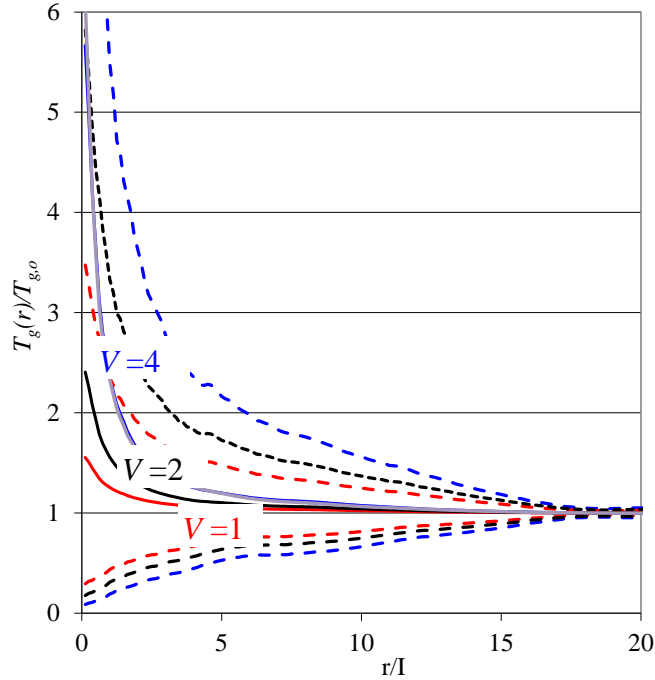
305 Figure 2. $T_g(r)$ as a function of radial distance for randomly selected transmissivity fields
 306 with $V=1$. $T_g(r)$ is normalized by the ensemble mean of T used in data generation. The
 307 distance r is normalized by the integral scale, I .

308

309 Figure 3 shows the expected value and upper/lower deciles of $T_g(r)$ for $V=1, 2$ and 4 . The
 310 expected value was computed for each distance r as the arithmetic average of the 1000
 311 realizations. Similar curves for other values of the variance could be developed readily.
 312 Analysis of the generated realizations shows that 1000 simulations were sufficient (with
 313 error less than 1%). Figure 3 shows that for $r=0$ the expected value is simply the arithmetic
 314 mean of the transmissivity at the well. For $r/I > 20$, $T_g(r)$ of each realization approaches the
 315 ensemble geometric mean and hence, the expected value over all realizations would also
 316 approach the ensemble geometric mean. The semi-variogram model selected influences the
 317 rate of change with distance, but not the end points.

318 Although Figure 3 depicts only the average and upper/lower deciles, it is evident that for a
 319 particular value of V and r/I , there is a range of possible values of $T_g(r)$. This range increases
 320 with the increase in the variance value, and decreases as r/I increases. This figure also shows
 321 overlap among the different set of curves; e.g., for a given distance, the possible range of
 322 values of T_g obtained with variance $V=2$ is fully comprised within the range spanned by $V=4$.

323 This overlap has an influence on the Bayesian estimation, as discussed in detail in section
 324 3.2.



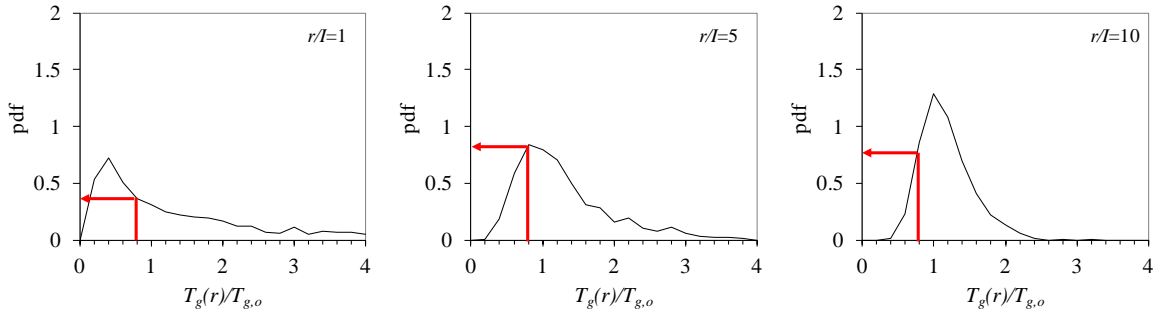
325
 326 Figure 3. Expected value (solid line) and upper/lower deciles (dashed lines) for $V=1, 2$ and
 327 4. The red, black and blue lines correspond to $V=1, 2$, and 4, respectively. $T_g(r)$ is normalized
 328 by the geometric mean of the transmissivity, $T_{g,o}$ used in data generation.

329
 330 Based on the information shown in Figure 3, it is possible to construct a distribution of all
 331 possible $T_g(r)$ values corresponding for each V and r/I pairs. Figure 4 shows the pdfs of $T_g(r)$
 332 at 3 different distances: $r/I=1, 5$ and 10, and for $V=1$. As distance increases, the statistical
 333 distribution becomes narrower and less skewed. It is important to note that these pdf's are
 334 computed only once and can be used in other problems provided the semi-variogram model
 335 is kept.

336 Figure 4 also shows a sample calculation of the likelihood function for a $T_g(r)$ obtained from
 337 a given pumping test. Starting from the $T_g(r)$ values derived from the pumping test, one can
 338 calculate the pdf corresponding for each V and I pairs. Because the pdf's depicted in Figure
 339 4 are for particular values of V and I , this calculation has to be repeated for all possible V
 340 and I pairs as defined by their prior joint distribution, $f_{v,i}(v, i)$.

341 According to the Bayesian formulation (Equation 4), the desired joint conditional pdf of V
 342 and I is function of the product of the likelihood function and the prior distribution. If for a

343 given pair (v, i) , the product of $f_{V,I}(v, i)$, and $f_T(T_{g,1} \cdots T_{g,N} | v, i)$ is small, the probability of
 344 the transmissivity field having these v and i values would also be small. On the other hand,
 345 if this product is large, this would mean that this (v, i) pair is more likely.
 346



347
 348 Figure 4: pdfs of $T_g(r)$ at $r/I=1, 5$ and 10 and for $V=1$. The red arrow represents the likelihood
 349 function for an example T value derived from a particular pumping test
 350

351 The above discussion illustrates the benefits of formulating the parameter estimation within
 352 a Bayesian framework. First, it incorporates the information inferred from the pumping test
 353 data, as well as any prior information about the site. Second, the Bayesian formulation
 354 simplifies the calculation by expressing the desired conditional pdf, $f_{V,I}^c(v, i | T_{g,1} \cdots T_{g,N})$ in
 355 terms of its reciprocal, $f_T(T_{g,1} \cdots T_{g,N} | v, i)$ (Eq. 4). Whereas the former can be viewed as a form
 356 of the inverse problem and its evaluation is not straight forward, $f_T(T_{g,1} \cdots T_{g,N} | v, i)$ can be
 357 readily determined from the randomly generated transmissivity fields corresponding to the
 358 v and i values as presented above without the need for any inverse modeling. Third, the
 359 Bayesian approach provides an estimate of the entire pdf based on prior information and the
 360 pumping test data and, as such, provides a measure of the uncertainty of the estimates.

361 In summary, we list below the main steps for the estimation of the conditional joint pdf of V
 362 and I , $f_{V,I}^c(v, i | T_{g,1} \cdots T_{g,N})$:

- 363 1. Given N pumping tests, the geometric transmissivity as a function of radial distance
 364 $T_{g,1}(r) \cdots T_{g,N}(r)$ is estimated using the CD method. Each pumping test is analyzed
 365 separately.
- 366 2. The prior joint pdf of V and I , $f_{V,I}(v, i)$, is defined based on prior information about the
 367 site.

- 368 3. For the available pumping tests, the likelihood function $f_T(T_{g,1} \cdots T_{g,N} | v, i)$ is determined
 369 from Figures 3 and 4. By assuming the pumping tests are sufficiently far and, therefore,
 370 can be treated as independent, the likelihood function is expressed as a product of the
 371 likelihood functions of the individual pumping tests (Eq. 6). It is important to note that
 372 these figures do not require the simulation of the groundwater flow equation; they were
 373 developed by generated multiple realizations of the transmissivity field and averaging
 374 the T as a function of radial distance. The calculation of the likelihood function is
 375 repeated for all possible v and i pairs as defined by their prior distribution (step 2).
- 376 4. The normalizing parameter, ω , is calculated from Eq. (5) or Eq. (7) if the pumping tests
 377 treated as independent.
- 378 5. The desired conditional pdf is finally computed according to Eq. (4) or Eq. (6). The
 379 marginal distributions of V and I are determined from Eq (8) and Eq. (9), respectively.
 380

381 **3. Application**

382 **3.1. Data Generation**

383 To demonstrate the above parameter estimation procedure, the procedure was tested using
 384 1000 synthetic pumping tests conducted in confined heterogeneous aquifers. The
 385 heterogeneous transmissivity fields were generated using the turning bands method. It was
 386 assumed that the natural log transform of the transmissivity is a multivariate Gaussian
 387 random spatial function with zero mean ($T_g=1$), an exponential semi-variogram, with
 388 variance, $V=1$, and integral scale, $I= 8$ length units (lu). Storativity was assumed to be
 389 uniform, as field data usually indicate that the spatial variation in storativity is less than that
 390 of the transmissivity. The storativity value used in all simulations was 0.0001; which is a
 391 typical value for a confined aquifers (*Domenico and Schwartz, 1997*).

392 The flow domain was assumed to be 481 by 481 lu. A fully penetrating pumping well was
 393 placed at the center of the domain. The observation point was assumed to be at a distance of
 394 $I/8$ from the pumping well. Constant head conditions were prescribed along the outer
 395 boundaries of the domain. The duration of the pumping test was $\tau=1$, while the pumping rate
 396 was fixed at $Q=2$ (using consistent units for both τ and Q). Pumping tests were terminated
 397 before the drawdown data were affected by boundary effects.

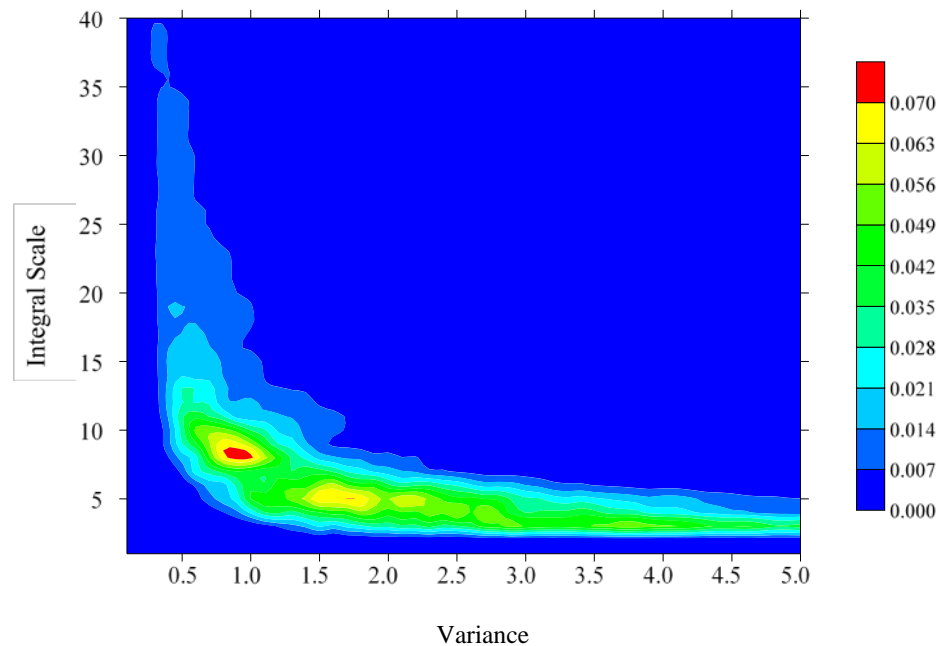
398 The pumping tests were simulated using MODFLOW (Harbaugh *et al.*, 2000). A uniform
 399 grid of 1 by 1 lu was used. The drawdown data were analyzed using the CD method yielding
 400 one $T_g(r)$ for each of the 1000 simulated pumping tests. Using the proposed Bayesian
 401 approach, the inferred $T_g(r)$ was then used to estimate the variance and integral scale. To
 402 assess the robustness of the proposed method, a Monte Carlo approach was adopted. First,
 403 each of the $T_g(r)$ curves were used independently to estimate the variance and integral scale
 404 of the T field. This corresponds to the case when only a single pumping test is present ($N=1$).
 405 The method was then repeated by combining 5 and 10 pumping tests ($N=5$ and $N=10$,
 406 respectively) to test the performance of the method when multiple wells are present.
 407 The Bayesian estimation requires the definition of a prior distribution for the parameters of
 408 interest (variance and integral scale). In the present analysis, the prior distribution of the
 409 variance was assumed to be uniform between 0 and 5, $U_V(0,5)$. This range encompasses
 410 typical variance values encountered in the field (Gelhar, 1993). The prior pdf of the integral
 411 scale was also assumed to be uniform between 0 and 40 lu, $U_I(0,40)$. The uniform
 412 distributions are the least informative distributions in terms of priors, requiring only the
 413 definition of upper limits (5 and 40 lu, respectively). The corresponding joint prior pdf is
 414 $f_{V,I}(v,i)=1/5 \times 1/40=0.005$. The joint pdf is also uniformly distributed which means that all v
 415 and i pairs falling between the lower and upper limits of V and I respectively have the same
 416 probability of occurring. To assess the sensitivity of the prior distribution on the estimation
 417 of the variance and integral scale, the analysis was also repeated assuming the prior
 418 distributions of the variance and the integral scale are $U_V(0,3)$ and $U_I(0,30)$, respectively,
 419 which are closer to the parameter values used in data generation.

420

421 **3.2. Results**

422 The parameter estimation procedure was repetitively applied to all 1000 pumping tests.
 423 Figure 5 shows a randomly selected example of the conditional joint pdf of the variance and
 424 integral scale obtained with the Bayesian estimation procedure. The true variance and
 425 integral scale used in the data generation are 1 and 8 lu, respectively. The number of available
 426 pumping tests was 5. The conditional pdf joint should be contrasted to the prior
 427 $f_{V,I}(v,i)=0.005$. This figure shows that conditioning on the pumping test data shifts the pdf
 428 from the diffuse prior towards the true values of the variance and integral scale ($v=1$, $i=8$ lu).
 429 The range of the more likely values of the variance and integral scale significantly decreased.

430



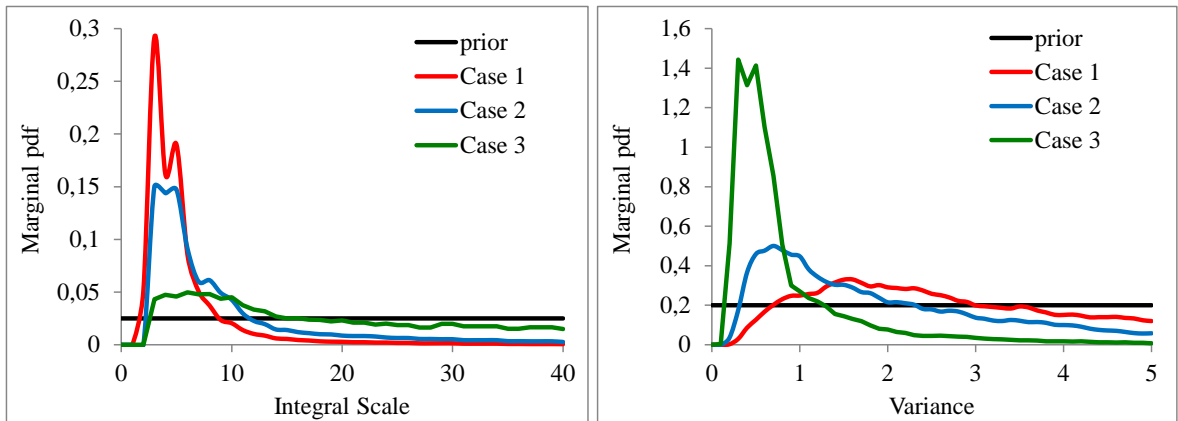
431

432 Figure 5. Example of the conditional joint pdf of the variance and integral scale based on
 433 data from 5 pumping tests. The prior distributions of the variance and integral scale are
 434 $U_V(0,5)$ and $U_I(0,40)$ which correspond to a prior pdf $f_{V,I}(v,i)=0.005$. The true values are
 435 $V=1$ and $I=8$ lu.

436

437 The marginal distributions of the integral scale and variance for 3 randomly selected cases
 438 are shown in Figure 6. Each of these conditional pdfs were computed assuming 5 pumping
 439 tests were available. The mean of the marginal pdfs of the integral scale for the three
 440 randomly selected cases were 5.8, 9.2 and 17 lu. The mean of the marginal pdfs of the
 441 variance on the other hand were 2.4, 1.8 and 0.86. For comparison, the prior pdfs of V and I
 442 are also shown in this figure. The corresponding means of the prior pdfs of the integral scale
 443 and variance were 20 lu and 2.5, respectively. These results show that the conditional
 444 variance and integral scale marginal pdfs are closer to the true values ($V=1$, $I=8$ lu) compared
 445 to the initial prior distribution. The conditional marginal pdfs do exhibit a tail that results
 446 from the diffuse prior distribution of V and I , and the overlap of the likelihood functions
 447 (Figures 3 and 4).

448



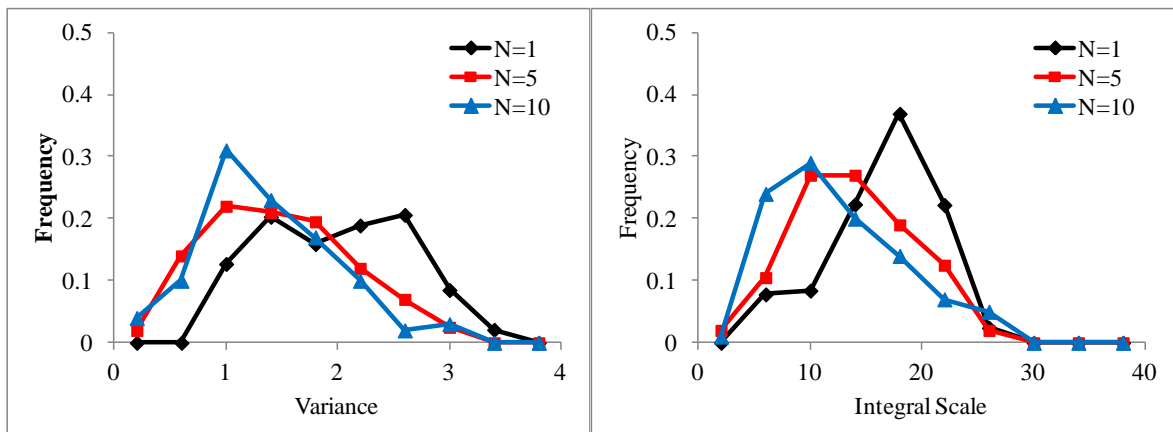
449

450 Figure 6. Integral scale and variance marginal pdfs for three randomly selected cases. Each
 451 of these cases assumes 5 pumping tests are available. The prior distributions of the
 452 variance and integral scale are $U_V(0,5)$ and $U_I(0,40)$. The true values are $V=1$ and $I=8$ lu.

453

454 Figure 7 presents the histogram of the conditional expected values of the integral scale ($E[I]$)
 455 and variance ($E[V]$), from the 1000 Monte Carlo results. The results are computed using 1,
 456 5 or 10 pumping tests. The average of $E[V]$ and $E[I]$ over all realization for $N=1, 5,$ and 10
 457 are shown in Table 1, For comparison, the “true” values of V and I used in the generation of
 458 the T fields and the expected values of the prior distribution are also included. Figure 7 and
 459 Table 1 demonstrate that the Bayesian updating can be viewed as a weighted average of the
 460 prior pdf and the results of the pumping test. Conditioning improves the estimation of the
 461 considered variables although, because of the overlap of the different likelihood functions
 462 (Figures 3), the resulting histograms still show some spread. Provided there is no redundancy
 463 in the data, increasing the number of pumping tests causes the estimates of the variance and
 464 integral scale to shift towards the true values.

465



466

467 Figure 7. Histograms of $E[V]$ and $E[I]$ based on the Monte Carlo analysis, assuming 1, 5 or
 468 10 pumping tests are available. The prior distributions are $U_V(0,5)$ and $U_I(0,40)$, implying
 469 expected values of 2.5 and 20 lu, respectively. The true values are $V=1$ and $I=8$ lu.

470

471 Table 1: Average of $E[V]$ and $E[I]$ for all simulations, assuming $N=1, 5$ or 10 pumping tests
 472 are available and for different prior distributions of the variance and integral scale. For
 473 comparison, the true values used in the generation of the transmissivity field are also shown

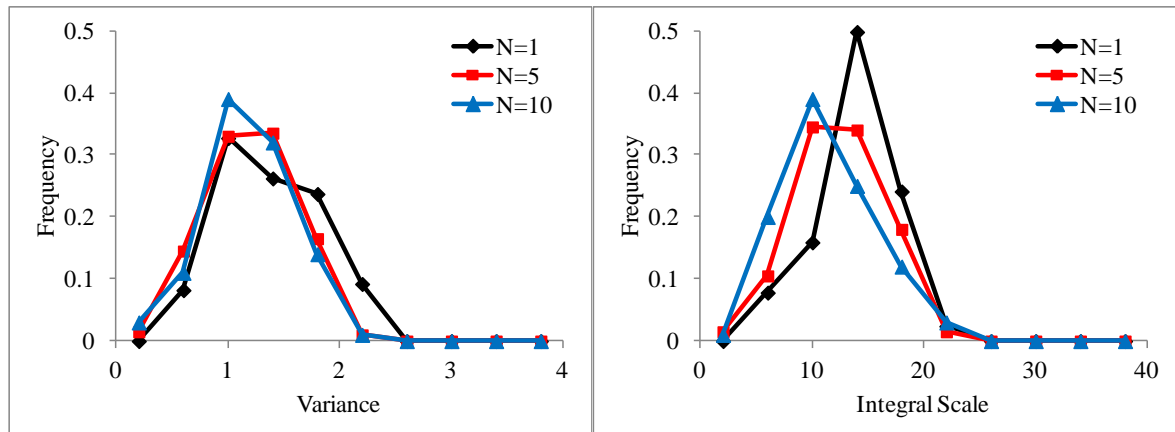
Prior distributions	Number of Pumping Tests	Average of $E[V]$	Average of $E[I]$, lu
V : Uniform between 0 and 5 I : Uniform between 0 and 40 lu	0	2.5	20
	1	1.96	16.7
	5	1.47	13.9
	10	1.36	12.4
V : Uniform between 0 and 3 I : Uniform between 0 and 30 lu	0	1.5	15
	1	1.36	13.8
	5	1.21	12.5
	10	1.17	11.5
"True" Values of I and V		1	8

474 Note: The average values corresponding to $N=0$ are the values of the prior distributions
 475 before conditioning on the pumping well data

476

477 To assess the impact of the prior V and I distributions, the parameter estimation procedure
 478 was repeated with the same pumping tests, but now assuming that the initial distributions of
 479 the variance and integral scales are uniformly distributed between 0 and 3 and between 0
 480 and 30 lu, respectively. Figure 8 shows the histograms of the $E[V]$ and $E[I]$ for different
 481 number of pumping tests. The corresponding average of $E[V]$ and $E[I]$ for all simulations are
 482 given in Table 1. With increase in the number of pumping tests, $E[V]$ and $E[I]$ move from
 483 the expected values of the prior distributions, $E^P[V] = 1.5$ and $E^P[I] = 15$ lu, towards the true
 484 parameter values, $V=1$ and $I=8$ lu. Compared to Figure 7, the impact of the number of tests
 485 on the estimation is less significant (in particular for $E[V]$), because the prior estimates were

486 closer to the true values. This demonstrates the benefits of using accurate prior distributions
 487 in Bayesian estimation procedures provided such information is available.
 488



489
 490 Figure 8. Histograms of $E[V]$ and $E[I]$, assuming 1, 5 or 10 pumping tests are available.
 491 The prior distributions are $U_V(0,3)$ and $U_I(0,30)$, implying expected values of 1.5 and 15 lu,
 492 respectively. The true values are $V=1$ and $I=8$ lu.
 493

494 4. Summary and Conclusions

495 Modeling of the spatial variability of transmissivity is essential for the accurate simulation
 496 of groundwater flow and contaminant transport. The spatial variability of T is commonly
 497 defined in terms of a semi-variogram or covariance function that is expressed in terms of
 498 two statistical parameters: the variance, V , and integral scale, I . It is therefore important to
 499 develop simple techniques for the estimation of these two statistical parameters. Despite the
 500 development in recent years of novel data acquisition techniques, the analysis of drawdown
 501 data from pumping tests remain the most commonly used technique for the identification of
 502 subsurface flow parameters. Traditionally, the interpretation of pumping tests generally yield
 503 single representative (apparent) estimates of the flow parameters. Here we explore whether
 504 pumping test data can be used to infer the variance and integral scale of the transmissivity,
 505 two statistical parameters that describe the spatial variability of the underlying transmissivity
 506 field. Estimates of the variance and integral scale can be employed in the analysis of flow
 507 and contaminant transport problems and their associated uncertainty, either directly using
 508 various analytical expressions found in the literature that relate flow and transport attributes

509 to the underlying aquifer heterogeneity, or numerically through the generation of multiple
510 realizations of the transmissivity field.

511 The starting point of the present study is the Continuous Derivation method (Coptý *et al.*,
512 2011), which uses the drawdown and its time derivative to estimate a function that was
513 shown to be close to the geometric mean of the transmissivity field defined over an
514 increasing radial distance from the pumping well, $T_g(r)$. Analysis of $T_g(r)$ indicated that the
515 early part of the curve is sensitive to the variance of the T field while the rate at which it
516 approaches the geometric mean of T in the full domain could be related to the integral scale.
517 This provided the basis for attempting to use $T_g(r)$ for estimating V and I .

518 The estimation of V and I was formulated using a Bayesian approach which expresses the
519 conditional pdf of V and I as a weighted function of the prior pdf and the likelihood function
520 that is itself dependent on the pumping test data. An important advantage of this approach is
521 that the likelihood function is readily computed from multiple realizations of the
522 transmissivity without the need to solve potentially complex inverse problems. Another
523 feature of the Bayesian approach is that it provides a measure of the uncertainty of the
524 estimated statistical parameters.

525 The Bayesian estimation procedure was applied to a number of synthetic pumping tests. The
526 analysis assumed that the natural log transform of the transmissivity distribution is a
527 multivariate Gaussian random spatial function with an exponential variogram. The variance
528 and integral scale were assumed to have a uniform joint prior distribution. The diffuse prior
529 distributions considered in this application and the non-uniqueness of the likelihood function
530 means that the results of the estimation procedure can be associated with a significant level
531 of uncertainty, highlighting the challenges of the parameter estimation problem. Single as
532 well as multiple pumping tests ($N=5$ and $N=10$) were assumed to be available. In the case
533 when multiple pumping tests were available, it was further assumed that they are located far
534 from each other such they sample different portions of the aquifer.

535 The significance of the Bayesian estimation procedure becomes apparent when the
536 conditional distribution of V and I is compared to the prior pdf of V and I which represents
537 the level of information available prior to conducting the pumping tests. It is shown that
538 improved estimates of V and I are obtained as the number of available pumping tests
539 increases or when more accurate prior distributions are available. The results of this
540 numerical example show that as little as 5 pumping tests may be sufficient to yield reliable
541 estimates of the statistical parameters of the transmissivity field.

542 Overall, the proposed interpretation procedure can be viewed as an extension of traditional
543 pumping test interpretation procedures, such as the Theis method, that besides best-fit
544 estimates of the storativity and transmissivity, can potentially also provide estimates of the
545 variance and integral scale of the transmissivity field.

546

547 **5. Acknowledgements**

548 Mehmet Taner Demir and Nadim Coptu acknowledge the financial support provided by the
549 Bogazici University Research Fund (BAP), Istanbul, Turkey (Project Number 6722).

550 Xavier Sanchez-Vila acknowledges support from the ICREA Academia Program. This paper
551 has benefited from helpful comments by Walter Illman and two anonymous reviewers.

552

553 **6. References**

554 Attinger, S., 2003. Generalized Coarse Graining Procedures for Flow in Porous Media,
555 *Computational Geosciences*, 7(4), 253-273,

556 Avci, C.B., Sahin, A.U., Ciftci, E., 2011. Aquifer Parameter Estimation Using an
557 Incremental Area Method, *Hydrological Processes*, 25(16), 2584–2596.

558 Avci, C.B., Sahin, A.U., Ciftci, E., 2013. A new method for aquifer system identification
559 and parameter estimation, *Hydrological Processes*, 27(17), 2485–2497.

560 Avci, C. B., Sahin, A.U., 2014. Assessing radial transmissivity variation in heterogeneous
561 aquifers using analytical techniques, *Hydrological Processes*, 28, 5739–5754.

562 Barker, J.A., Herbert, R., 1982. Pumping tests in patchy aquifers. *Ground Water*, 20, 150–
563 155.

564 Binley, A., Hubbard, S.S., Huisman, J.A., Revil, A., Robinson, D.A., Singha, K., Slater,
565 L.D., 2015. The emergence of hydrogeophysics for improved understanding of
566 subsurface processes over multiple scales, *Water Resour. Res.*, 51, 3837–3866,
567 doi:10.1002/2015WR017016.

568 Bohling, G.C., and Butler Jr., J.J., 2010. Inherent limitations of hydraulic tomography.
569 *Ground Water* 48(6), 809–824.

- 570 Bohling, G.C., Liu, G., Knobbe, S.J., Reboulet, E.C., Hyndman, D.W., Dietrich, P., Butler,
571 J.J., 2012. Geostatistical analysis of centimeter-scale hydraulic conductivity
572 variations at the MADE site, *Water Resour. Res.*, 48, W02525,
573 doi:10.1029/2011WR010791.
- 574 Bourdet, D., 2002. *Well Test Analysis: The Use of Advanced Interpretation Models*, Elsevier,
575 Amsterdam, Boston.
- 576 Butler Jr., J.J., 1988. Pumping tests in nonuniform aquifers - The radially symmetric case.
577 *Journal of Hydrology*, 101, 15–30.
- 578 Butler Jr., J.J. 1990. The role of pumping tests in site characterization: some theoretical
579 considerations, *Ground Water*, 28(3), 394-402.
- 580 Butler Jr., J.J., McElwee, C.D., Bohling G. C. 1999. Pumping tests in networks of multilevel
581 sampling wells: Motivation and methodology, *Water Resour. Res.*, 35(11), 3553-
582 3560, doi:10.1029/1999WR900231.
- 583 Butler Jr., J.J., Dietrich, P., Wittig, V., Christy T., 2007. Characterizing hydraulic
584 conductivity with the direct-push permeameter, *Ground Water*, 45(4), 409-419.
- 585 Cooper, H., Jacob C., 1946. A generalized graphical method for evaluating formation
586 constants and summarizing well-field history, *Trans., Am. Geophys. Union*, 27(4),
587 526-534.
- 588 Coptly, N.K., Findikakis A.N., 2004a. Stochastic analysis of pumping test drawdown data in
589 heterogeneous geologic formations, *J. Hydraul. Res.*, 42, 59-67.
- 590 Coptly, N.K., Findikakis A.N., 2004b. Bayesian identification of the local transmissivity
591 using time-drawdown data from pumping tests, *Water Resour. Res.*, 40, W12408,
592 doi:10.1029/2004WR003354.
- 593 Coptly, N.K., Trinchero, P., Sarioglu, M.S., Findikakis, A.N., Sanchez-Vila, X., 2008.
594 Influence of heterogeneity on the interpretation of pumping test data in leaky
595 aquifers, *Water Resour. Res.*, 44, W11419, doi:10.1029/2008WR007120
- 596 Coptly, N.K., Trinchero, P., Sanchez-Vila, X., 2011. Inferring spatial distribution of the
597 radially integrated transmissivity from pumping tests in heterogeneous confined
598 aquifers, *Water Resour. Res.*, 47 (5). W05526, doi:10.1029/2010WR009877.

- 599 Delay, F., Ackerer, P., Belfort, B., Guadagnini, A., 2012. On the emergence of reciprocity
600 gaps during interference pumping tests in unconfined aquifers, *Adv. Water Resour.*,
601 46, 11–19, doi:10.1016/j.advwatres.2012.06.002.
- 602 Dietrich P., Butler, J.J. Jr, Faiss, K., 2008. A rapid method for hydraulic profiling in
603 unconsolidated formations., *Ground Water*, 46(2), 323-328.
- 604 Feitosa, G.S., Chu L., Thompson, L.G., Reynolds, A.C., 1994. Determination of
605 permeability distribution from well test pressure data. *Society of Petroleum*
606 *Engineers*, 26: 407.
- 607 Firmani, G., Fiori, A., Bellin, A., 2006. Three-dimensional numerical analysis of steady state
608 pumping tests in heterogeneous confined aquifers, *Water Resour. Res.*, 42, W03422,
609 doi:10.1029/2005WR004382
- 610 Gelhar, L.W., 1993. *Stochastic Subsurface Hydrology*, Prentice-Hill, 643 Upper Saddle
611 River, N. J.
- 612 Harbaugh, A.H., Banta, E.R., Hill, M.C., McDonald, M.G., 2000. MODFLOW-2000, The
613 U.S. Geological Survey Modular Ground-Water Model- User Guide to
614 Modularization Concepts and the Ground-Water Flow Process, U.S. Geological
615 Survey, Open-File Report 00-92.
- 616 Illman, W.A., Berg, S.J., Zhao Z., 2015. Should hydraulic tomography data be interpreted
617 using geostatistical inverse modeling? A laboratory sandbox investigation, *Water*
618 *Resour. Res.*, 51, doi:10.1002/ 2014WR016552
- 619 Kitanidis, P.K., 1997. *Introduction to Geostatistics: With Applications in Hydrogeology*,
620 Cambridge University Press, New York.
- 621 Knight, J., Kluitenberg, G., 2005. Some analytical solutions for sensitivity of well tests to
622 variations in storativity and transmissivity, *Adv. in Water Res.*, 28 (10), 1057-1075,
- 623 Leven, C., Dietrich, P., 2006. What information can we get from pumping tests? comparing
624 pumping test configurations using sensitivity coefficients, *J. Hydrol.*, 319 (14), 199-
625 215.
- 626 Mantoglou, A., Wilson J.L, 1982. The turning bands method for simulation of random-fields
627 using line generation by a spectral method, *Water Resour. Res.*, 18(5), 1379-1394.
- 628 Meier, P.M., Carrera, J., Sanchez-Vila, X., 1998. An evaluation of Jacob's method for the
629 interpretation of pumping tests in heterogeneous formations, *Water Resour. Res.*,
630 34(5), 1011-1025.

- 631 Neuman, S.P., Guadagnini, A., Riva, M., 2004. Type-curve estimation of statistical
632 heterogeneity, *Water Resour. Res.*, 40, W04201, doi:10.1029/2003WR002405.
- 633 Neuman, S.P., Blattstein, A., Riva, M., Tartakovsky, D.M., Guadagnini, A., Ptak, T., 2007.
634 Type curve interpretation of late-time pumping test data in randomly heterogeneous
635 aquifers, *Water Resour. Res.*, 43, W10421, doi:10.1029/2007WR005871
- 636 Oliver, D.S. 1993. The influence of nonuniform transmissivity and storativity on drawdown,
637 *Water Resour. Res.*, 29(1), 169-178, 1993.
- 638 Pechstein, A., Attinger, S., Krieg, R., Coptly, N.K., 2016. Estimating transmissivity from
639 single-well pumping tests in heterogeneous aquifers, *Water Resour. Res.*, 52(1), 495-
640 510
- 641 Renard, P., 2007. Stochastic hydrogeology: what professionals really need? *Ground Water*,
642 45, 531-541.
- 643 Riva, M., Guadagnini, A., Bodin, J., Delay, J., 2009. Characterization of the hydrogeological
644 experimental site of Poitiers (France) by stochastic well testing analysis, *J. Hydrol.*,
645 369(1-2), 154-164.
- 646 Rubin, Y., 2003. *Applied Stochastic Hydrogeology*, Oxford University Press. New York.
- 647 Rubin, Y., Hubbard, S., 2005. *Hydrogeophysics*, Series: Water Science and Technology
648 Library, 50, Springer.
- 649 Sanchez-Vila, X., Ackerer, P., Delay, F., Guadagnini, A., 2016. Characterization of
650 reciprocity gaps from interference tests in fractured media through a dual porosity
651 model, *Water Resour. Res.*, 52, doi:10.1002/2015WR018171.
- 652 Sanchez-Vila, X., Fernández-García, D., 2016. Debates-Stochastic subsurface hydrology
653 from theory to practice: Why stochastic modeling has not yet permeated into
654 practitioners?, *Water Resour. Res.*, 52, 9246–9258, doi:10.1002/2016WR019302.
- 655 Sanchez-Vila, X., Guadagnini, A., Carrera, J., 2006. Representative hydraulic conductivities
656 in saturated groundwater flow, *Rev. Geophys.*, 44(3), RG3002.
- 657 Sanchez-Vila, X., Meier, P.M., Carrera, J., 1999. Pumping tests in heterogeneous aquifers:
658 An analytical study of what can be obtained from their interpretation using Jacob's
659 method, *Water Resour. Res.*, 35(4), 943–952.
- 660 Slater, S., 2007. Near surface electrical characterization of hydraulic conductivity: from
661 petrophysical properties to aquifer geometries—A review, *Surv Geophys* 28, 169–
662 197, doi:10.1007/s10712-007-9022-y

- 663 Sudicky, E.A., Illman, W.A., Goltz, I.K., Adams, J.J., McLaren, R.G., 2010. Heterogeneity
664 in hydraulic conductivity and its role on the macroscale transport of a solute plume:
665 From measurements to a practical application of stochastic flow and transport theory,
666 *Water Resour. Res.*, 46, W01508, doi:10.1029/2008WR007558.
- 667 Tarantola, A., 1987. *Inverse Problem Theory, Methods for Data Fitting and Model*
668 *Parameter Estimation*, Elsevier Science Publishers, Amsterdam, Holland.
- 669 Theis, C.V., 1935. The relation between the lowering of the piezometric surface and the rate
670 and duration of discharge of a well using groundwater storage, *Trans., Am. Geophys.*
671 *Union*, 16, 519– 524.
- 672 Trinchero, P., Sanchez-Vila, X., Coptly, N.K., Findikakis, A.N., 2008a. A new method to
673 interpret pumping tests in leaky aquifers, *Ground Water*, 46(1), 133-143.
- 674 Trinchero, P., Sanchez-Vila, X., Fernandez-Garcia, D., 2008b. Point-to-point connectivity,
675 an abstract concept or a key issue for risk assessment studies?, *Adv. Water Resour.*,
676 31(12), 1742-1753.
- 677 Yeh, T.C.J., Liu, S., 2000. Hydraulic tomography: Development of a new aquifer test
678 method, *Water Resour. Res.*, 36(8), 2095– 2105.
- 679 Yin, D. T., Illman, W.A., 2009. Hydraulic tomography using temporal moments of
680 drawdown recovery data: A laboratory sandbox study, *Water Resour. Res.*, 45, Art.
681 No. W01502.
- 682 Zech, A., Schneider, C.L., Attinger, S., 2012. The Extended Thiem's solution: Including the
683 impact of heterogeneity, *Water Resour. Res.*, 48 (10), W10,535.
- 684 Zech, A., Arnold, S., Schneider, C.,L., Attinger, S., 2015. Estimating Parameters of Aquifer
685 Heterogeneity Using Pumping Tests - Implications for Field Applications, *Adv.*
686 *Water Resour.*, 38,137–147.
- 687 Zech, A., Müller, S., Mai, J., Heße, F., Attinger S., 2016. Extending Theis' solution: Using
688 transient pumping tests to estimate parameters of aquifer heterogeneity, *Water*
689 *Resour. Res.*, 52, 6156–6170, doi:10.1002/2015WR018509.
- 690 Zhu, J., Yeh, T.J., 2005. Characterization of aquifer heterogeneity using transient hydraulic
691 tomography, *Water Resour. Res.*, 41, W07028, doi:10.1029/2004WR003790.